

Chapter 2

Origin of Lateral Heterogeneities in the Upper Mantle Beneath South-east Australia from Seismic Tomography

N. Rawlinson, B.L.N. Kennett, M. Salmon and R.A. Glen

Abstract We use teleseismic body wave tomography to reveal anomalous P wave velocity variations in the upper mantle beneath south-east Australia. Data are sourced from the WOMBAT transportable seismic array, the largest of its kind in the southern hemisphere, which enables horizontal resolution of approximately 50 km to be achieved over a large region that includes Victoria, New South Wales and southern South Australia. In order to account for long-wavelength structure that is lost due to the use of multiple teleseismic datasets from adjacent arrays with non-overlapping recording periods, the AuSREM mantle model is included as prior information in the inversion. Furthermore, AuSREM crust and Moho structure is explicitly included in the initial model in order to account for the presence of shallow heterogeneity which is poorly constrained by the teleseismic dataset. The P wave velocity model obtained from the joint inversion of WOMBAT teleseismic data represents a vast new resource on the seismic structure of the upper mantle beneath south-east Australia. One of the most striking features of the model is the presence of a north-dipping low-velocity anomaly beneath the Newer Volcanics province, a Quaternary intraplate basaltic province in western Victoria. The anomaly appears to terminate at approximately 200 km depth and has a structure that is more suggestive of a source confined to the upper mantle rather

N. Rawlinson (✉)

School of Geosciences, University of Aberdeen, Aberdeen AB24 3UE, Scotland
e-mail: nrawlinson@abdn.ac.uk

B.L.N. Kennett · M. Salmon

Research School of Earth Sciences, The Australian National University,
Canberra, ACT 0200, Australia
e-mail: brian.kennett@anu.edu.au

M. Salmon

e-mail: michelle.salmon@anu.edu.au

R.A. Glen

Geological Survey of New South Wales, NSW Department of Trade and Investment,
Maitland, NSW 2310, Australia
e-mail: dick.glen@industry.nsw.gov.au

than a deeply rooted mantle plume. Other features that can be observed include a high-velocity anomaly beneath the Curnamona province and a high-velocity salient beneath the New England Orogen. Of particular interest is an extensive high-velocity anomaly beneath the Lachlan Orogen, which coincides almost exactly with the surface expression of the Hay–Booligal Zone in the south, and extends northwards beneath the Macquarie Arc. The higher velocities beneath the Hay–Booligal Zone are consistent with the idea that it may be floored by a fragment of Proterozoic continental lithosphere that was once part of the east Gondwana margin, while the higher velocities beneath the Macquarie Arc may be related to its origin as an intra-oceanic arc.

Keywords Australia • Continental lithosphere • Seismic tomography • Accretionary orogen • Gondwana

2.1 Introduction

The seismic structure of the upper mantle beneath Australia has been progressively revealed over the last half century using a variety of passive and active source techniques. Some of the earliest measurements of mantle velocities come from recordings of nuclear tests undertaken by the British Atomic Weapons Research Establishment in South Australia (Doyle 1957; Bolt et al. 1958). As a result of the foresight of Sir Edward Bullard and Prof. John Jaeger, seven seismometers were placed along a transect that followed the Trans-Australian railway westwards away from the test site at Maralinga out to an angular distance of nearly 11° towards Perth. This allowed refraction and wide-angle reflection phases generated by the nuclear explosions to be recorded and analysed. Doyle (1957) used simple refraction analysis that assumed lateral homogeneity to estimate Pg (6.12 km/s), Sg (3.56 km/s), Pn (8.23 km/s), Sn (4.75 km/s) and Moho depth (35–40 km) beneath cratonic central and Western Australia.

In the mid-1960s, active sources were again used to interrogate crust and upper mantle structure when obsolescent depth charges were exploded on the sea floor beneath Bass Strait as part of BUMP (Bass Strait Upper Mantle Project). Using recording stations in Tasmania and mainland Australia, Underwood (1969) and Johnson (1973) exploited the move-out characteristics of refraction and wide-angle reflection phases to show that the Moho varied in depth from 37 km beneath the Snowy Mountains in New South Wales, to 25 km beneath Bass Strait and to 30–35 km beneath Tasmania, with an average Pn velocity of 7.8 km/s. Despite the use of relatively low fidelity equipment (by modern standards), analogue records and simple methods of analysis that relied on several major assumptions (e.g. constant velocity crust), these early measurements are at a very broad scale consistent with more recent results; in particular that the P wave velocity of the upper mantle beneath south-east Australia is markedly lower than that of cratonic central and Western Australia (Kennett and Salmon 2012).

Following the early work described above, active source seismology began to be used more widely, although largely with a view to constraining crustal structure. However, measurements of mantle velocities were still made if the sources were large enough (e.g. Finlayson et al. 1974). Over time the use of explosive sources was gradually replaced with vibroseis and marine airguns. Although still capable of penetration into the upper mantle, most studies confined analysis of the mantle to measurement of Pn and in some cases vertical P wave velocity gradient (Finlayson et al. 1980, 1984, 1998; Rawlinson et al. 2001). As such, it is probably fair to say that most of our current knowledge of upper mantle seismic structure beneath south-east Australia has come from passive seismic imaging. Early studies tended to use surface wave recordings and measure basic properties such as path average group and phase velocities over a number of frequency bands (e.g. De Jersey 1946; Bolt and Niazi 1964). More complete dispersion analysis and inversion for 1-D shear-wave models soon followed (Thomas 1969). The advent of digital seismographs and more powerful computing facilities allowed increasingly sophisticated models of the upper mantle beneath Australia to be constructed (Lambeck and Penny 1984; Bowman and Kennett 1990, 1993; Kennett and Bowman 1990), although it was not until the continent-wide SKIPPY project (van der Hilst et al. 1994) that a coherent picture of the Australian mantle began to emerge.

SKIPPY was a transportable array project that can be regarded as the progenitor of both USArray and WOMBAT. It used a moveable array of broadband seismometers to gradually achieve continent-wide coverage of Australia with a station spacing of approximately 400 km, sufficient to record the large number of surface wave paths from regional events required for 3-D surface wave tomography. The SKIPPY dataset, plus data collected by subsequent more targeted arrays placed in regions of particular geological interest, has formed the basis for many surface wave studies of the Australian region over the last two decades (Zielhuis and van der Hilst 1996; Debayle 1999; Simons et al. 1999, 2002; Debayle and Kennett 2000; Yoshizawa and Kennett 2004; Fishwick et al. 2005, 2008; Fishwick and Rawlinson 2012). These results have proven instrumental in gaining a first-order understanding of the heterogeneous mantle structure beneath the Australian continent, with one of the principal outcomes being the ability to discriminate between older Precambrian shield regions of Australia and younger Phanerozoic terranes (Kennett et al. 2004), much of which are masked by younger sediments. Continent-wide body wave studies of the Australian mantle have also been carried out using the same dataset and include velocity tomography (Kennett 2003; Kennett et al. 2004), attenuation tomography (Kennett and Abdullah 2011), receiver functions (Clitheroe et al. 2000; Reading and Kennett 2003) and shear wave splitting (Heintz and Kennett 2005).

The goal of this paper is to illuminate the upper mantle beneath south-east Australia using teleseismic data from the WOMBAT transportable array and attempt to explain the origins of the lateral heterogeneities that are observed. To date, WOMBAT has involved 15 contiguous array deployments over the last 15 years and has achieved cumulative coverage of most of Tasmania, Victoria,

New South Wales and southern South Australia with approximately 650 sites and interstation spacings varying from 15 km in Tasmania to 50 km on mainland Australia. Compared to the continent-wide broadband experiments discussed above, WOMBAT passive seismic data have the potential to resolve much finer-scale variations in mantle structure, as has been demonstrated over the last decade by a number of teleseismic body wave studies (Graeber et al. 2002; Rawlinson et al. 2006a, b, 2010b, 2011; Rawlinson and Urvoy 2006; Clifford et al. 2008; Rawlinson and Kennett 2008; Rawlinson and Fishwick 2012; Fishwick and Rawlinson 2012). The current study differs from those that precede it by using a much larger dataset that includes recent arrays from northern New South Wales and southern South Australia, and explicitly accounting for near surface unresolved crust and Moho structure via inclusion of the recently released AuSREM (Australian Seismological Reference Earth Model) model.

2.1.1 Tectonic Setting

The WOMBAT array overlies the southern half of the Tasmanides, a complex series of Palaeozoic—early Mesozoic orogens that formed along the eastern margin of Gondwana during the retreat of the Pacific plate and encroaches onto the eastern edge of cratonic central and Western Australia (Figs. 2.1 and 2.3). The current state of knowledge on how this region of the Australian plate evolved is well described by a number of recent papers (e.g. Foster et al. 2009; Glen et al. 2009, 2012; Cayley 2011; Gibson et al. 2011; Glen 2013), so the brief overview given here will only focus on aspects that are particularly relevant to this study.

One view of the Tasmanides is that it progressively formed along a monotonically eastward rolling Pacific plate, which is consistent with its largely south-west–north-east younging direction (Foster and Gray 2000; Spaggiari et al. 2003, 2004; Foster et al. 2009). However, others have argued for alternative scenarios which involve significant continental transform faults (Glen et al. 1992; VandenBerg 1999) and the presence of sizable fragments of Precambrian continental crust (Cayley et al. 2002, Cayley 2011; Glen et al. 2012), relics of the break-up of the supercontinent Rodinia. In a recent paper, Glen (2013) argues that the palaeo-Pacific plate was segmented, with major transform faults propagating into the Tasmanides and leading to the formation of supra-subduction zone systems, which are bounded to the north and south by these faults. The differential rollback implied by this model explains why Palaeozoic orogenesis in the south (eastern South Australia, Victoria and New South Wales) occurred over a plate margin-perpendicular distance of over 1500 km, compared to only a few hundred km in the north. The transform faults which segment the palaeo-Pacific plate may manifest as E–W trending accommodation zones, one candidate being the curvilinear east–west trending structures at the southern margin of the Thomson Orogen.

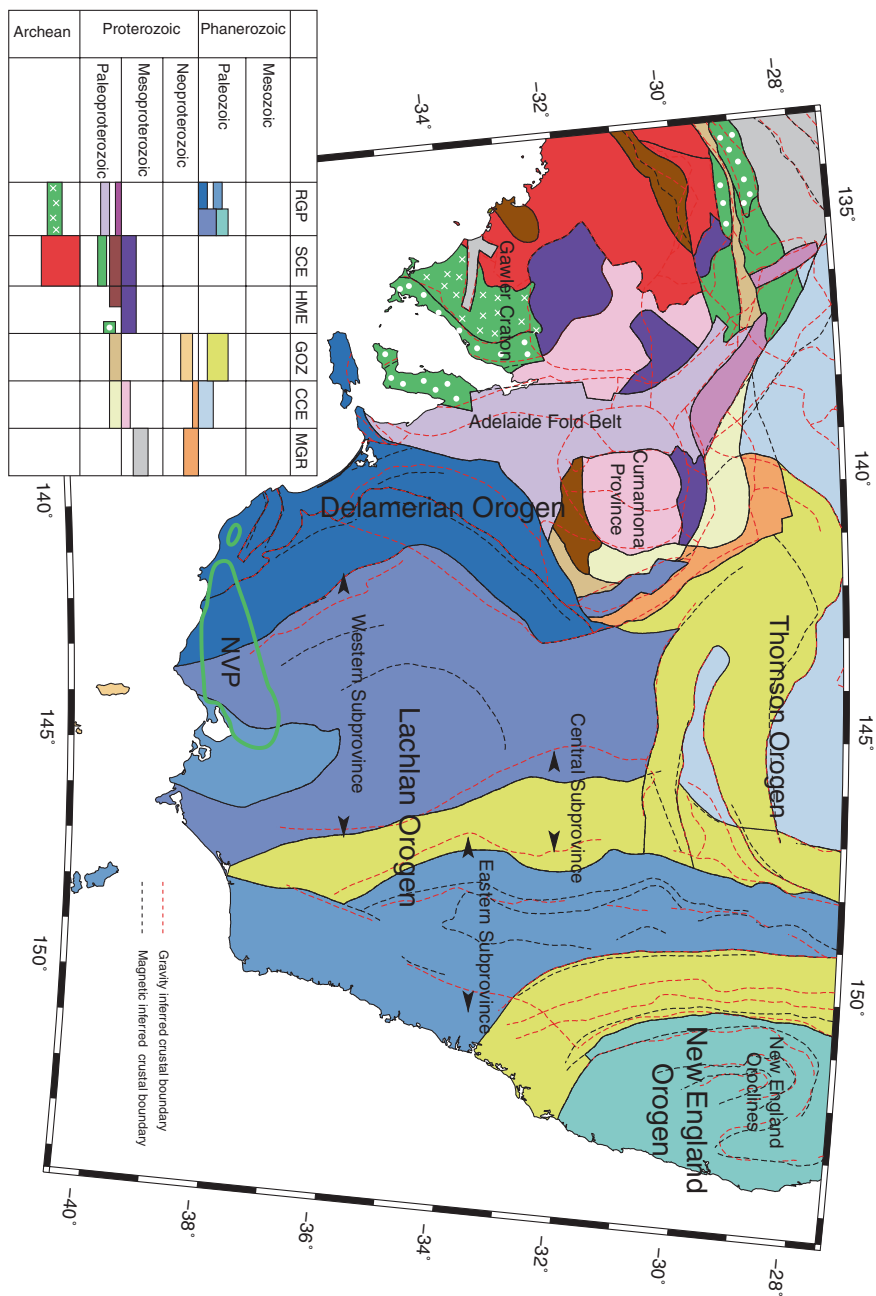


Fig. 2.1 The crustal elements of south-east Australia, as inferred from potential field data (based on data contained in Shaw et al. 1996). *RGP* relict geophysical pattern; *SCE* standard crustal element; *HME* highly magnetic element; *GOZ* geophysically overprinted zone; *CCE* covered crustal element; *MGR* subelement with muted geophysical response (see Shaw et al. 1996 for more details). *NVP* Newer Volcanics province. *Thick green line* denotes approximate surface expression of NVP

Precambrian continental fragments within the Tasmanides have proven difficult to identify and delineate, partly due to the extensive Mesozoic and Cenozoic sedimentary cover sequences that mask large regions of the Tasmanides. However, if present, one may expect them to have a distinctive seismic signature in the upper mantle provided that the subcrustal component of the lithosphere has not been delaminated post-emplacement. Previous seismic studies of the Australian plate (e.g. Zielhuis and van der Hilst 1996; Debayle and Kennett 2000; Fishwick et al. 2005; Fishwick and Rawlinson 2012) show that older, colder and depleted upper mantle beneath cratonic central and Western Australia is distinctly faster than the younger lithospheric mantle of Phanerozoic provenance. One candidate for a Precambrian continental fragment is the so-called Selwyn Block, which is inferred to lie underneath central Victoria, and is postulated to be an exotic Proterozoic microcontinental block—overlain by Cambrian greenstones—that collided with east Gondwana in the Late Cambrian (Cayley et al. 2002; Cayley 2011), possibly terminating the Delamerian Orogeny, the oldest orogenic belt in the Tasmanides. Based on evidence from magnetic and seismic reflection data, the Selwyn Block is thought to extend southwards beneath Bass Strait, where it forms the Proterozoic core of western Tasmania. The relative lack of Precambrian outcrop in the mainland Tasmanides has led researchers to explore various allochthonous models for the existence of a Proterozoic Tasmania, of which the Selwyn Block is but one. For example, Li et al. (1997) suggest that west Tasmania may be a by-product of Rhodanian break-up, while Calvert and Walter (2000) propose that King Island, and probably west Tasmania, rifted away shortly after 600 Ma. Other researchers to develop scenarios in which Tasmania existed as a separate continental block outboard of the Gondwana margin before becoming re-attached in the early Palaeozoic include Foster et al. (2005), Berry et al. (2008).

Another candidate Precambrian continental fragment is the core of the southern New England Orogen (Glen 2005, 2013), which lies inland of the eastern seaboard of northern New South Wales (Fig. 2.1). Although there is no outcrop, evidence drawn from active and passive seismic imaging (Finlayson 1993; Fishwick et al. 2008), geochemical data (Powell and O'Reilly 2007) and geochronology (Shaw et al. 2011) are suggestive of the presence of Proterozoic lower crust and lithospheric mantle, possibly within the framework of an emplaced microcontinental block. Largely on the basis of potential field data, Hallet et al. (2005) infer the presence of the so-called Hay–Booligal Block beneath the Murray Basin in southern New South Wales, which others have inferred to be a possible rifted fragment from the Curnamona province to the west (Glen 2013). Although somewhat speculative, the oroclinal wrapping of Ordovician to Cambrian strata around this region distinguishes it from other parts of the Lachlan Orogen. Another possible Precambrian continental fragment was recently identified by Glen et al. (2013) beneath the southern margin of the Thomson Orogen, which is heavily masked by sediments. On the basis of deep seismic reflection data, supported by potential field data and inferences from zircon measurements, they infer that a sliver of continent became stranded during the Neoproterozoic rifting of Rodinia and now sits juxtaposed against Palaeozoic oceanic crust to the north (Thomson Orogen) and to the south (Lachlan Orogen).

Despite many attempts, the boundary between the Australian craton and the Tasmanides—often referred to as the Tasman Line—has proven difficult to identify (Hill 1951; Scheibner 1974; Wellman 1976; Shaw et al. 1996; Scheibner and Veevers 2000; Li 2001), partly due to the presence of younger cover sequences which mask the Palaeozoic and Precambrian basement, and partly due to differences in definition (Direen and Crawford 2003). For instance, is the onset of the Tasmanides defined by the earliest Palaeozoic basin systems, the westernmost limit of deformation associated with Palaeozoic fold belts, or the onset of Palaeozoic oceanic substrate? Direen and Crawford (2003) discuss many attempts at defining a Tasman Line, and come to the conclusion that the various geophysical signatures present cannot be explained by the presence of a simple boundary and that attempts to define a Tasman Line should be abandoned. Passive seismic data have played a role in helping to understand the transition from cratonic Australia to the Tasmanides; for example, Kennett et al. (2004) carry out a synthesis of surface wave and body wave tomography and find a strong wavespeed contrast in the mantle beneath eastern and central Australia, which can be interpreted as a change from Precambrian cratonic to Palaeozoic lithosphere. However, they also found that the transition from one region to the other varied in complexity across strike and showed that the various interpretations of the Tasman Line coincide with different aspects of the mantle structures that are present.

The region under consideration in this study (see Figs. 2.1 and 2.3) crosses from the Tasmanides in the east into cratonic central Australia. In Fig. 2.1, the Delamerian Orogen represents the western most orogen of the Tasmanides and incorporates the Adelaide fold belt, Curnamona province and Kanmantoo fold belt. The Adelaide fold belt was formed by inversion of the Neoproterozoic–Cambrian Adelaide Rift Complex (Glen 2005; Foden et al. 1999, 2006), while the Curnamona province was thought to have been originally connected to the Gawler Craton prior to the Neoproterozoic (Belousova et al. 2006; Hand et al. 2008; Wade et al. 2012). Although originally regarded as cratonic (Thomson 1970), the Curnamona province underwent Middle-to-Late Cambrian deformation and metamorphism associated with the Delamerian Orogeny (e.g. Conor and Preiss 2008). The Kanmantoo fold belt developed from the inversion of the deep water Kanmantoo Trough (Glen 2005). The basement to the Delamerian Orogen appears to comprise reworked Precambrian continental rocks (Direen and Crawford 2003), although a transition to Palaeozoic oceanic crust beneath the south-east region of the orogen has been inferred (Glen 2013). Previous teleseismic studies of the region (e.g. Graeber et al. 2002; Rawlinson and Fishwick 2012) indicate that the lithospheric mantle beneath the Delamerian Orogen is characterized by higher velocities than that beneath the Lachlan Orogen, which is thought to be largely floored by Oceanic crust (Foster et al. 2009; Glen 2013).

Although the orogenic cycles that gave rise to the Tasmanides were largely complete by 227 Ma (Glen 2005), several subsequent tectonic events have significantly affected the nature of the mantle beneath south-east Australia. The main change was the termination of subduction off the eastern margin of Australia at about 100 Ma (Glen 2013) followed by the break-up of Australia and Antarctica,

and the opening of the Tasman Sea around 80–90 Ma (Gaina et al. 1998), which resulted in significant lithospheric thinning towards the passive margins and the formation of the Bass Basin as a result of failed intracratonic rifting (Gunn et al. 1997). The Southern Highlands, which are located in eastern New South Wales and Victoria and have a maximum elevation of over 2 km, may have formed as a result of the rifting process, although the exact timing and uplift mechanism remain a subject of debate. For example, if the eastern Australian passive margin formed as a result of asymmetric rifting, uplift beneath the upper plate margin is expected due to delamination of the mantle lithosphere (Lister et al. 1986, 1991; Lister and Etheridge 1989). However, others have argued that the Southern Highlands are the remnants of an older Palaeozoic Orogen (Lambeck and Stephenson 1986; van der Beek et al. 1999).

The widespread coverage of Cenozoic volcanism along the eastern seaboard of the Australian continent (Johnson 1989) has undoubtedly had an impact on the composition and thermal structure of the upper mantle in this region. The cause of this volcanism is often attributed to the so-called East Australia Plume System (Wellman 1983; Sutherland 1983), the origin of which lies offshore, but has been linked to 65 Ma rifting of the Coral Sea (Sutherland 1983). It was most active after 35 Ma and gets progressively younger further south in a manner that is consistent with the northward movement of the Australian continent over stationary hot spots. However, a consensus on the mechanism of formation has yet to be reached, with alternatives including mantle upwelling associated with slab detachment and temporal variations in crustal stresses coupled with underlying mantle convection (see Sutherland et al. 2012, for an overview).

The most recent example of Cenozoic volcanism in Australia occurs in western Victoria and south-east South Australia, where the Newer Volcanics province (NVP) contains evidence of eruptive activity that is less than 5 ka (Johnson 1989). Compared to the Cenozoic volcanic chains that populate the eastern seaboard of Australia, the NVP is unique in that it has not migrated over time. Moreover, it appears that the NVP is the latest phase of an eruption cycle that has operated intermittently since the early Eocene when fast northern motion of the Australian continent commenced (Demidjuk et al. 2007). Coupled with modest surface topographic response (~ 100 m) and a relatively low eruption volume ($\sim 20,000$ km³) researchers have begun to suspect that the source of the NVP does not fit the mould of a traditional mantle plume model, but instead may be a phenomenon localized to the upper mantle (Demidjuk et al. 2007; Rawlinson and Fishwick 2012).

2.1.2 AuSREM Model

The AuSREM represents a synthesis of structural information on the Australian lithosphere that has been derived from various active and passive source seismic imaging experiments over the last few decades (Kennett and Salmon 2012; Kennett et al. 2013, Salmon et al. 2012). AuSREM defines seismic structure on a

0.5° grid in both latitude and longitude, with depth variations determined by major boundaries such as the Moho and sediment-basement interface, and information obtained from smooth tomographic models. P and S wavespeed as well as density is defined in the crust, mantle lithosphere and sublithospheric mantle to a depth of 350 km. Laterally, the crustal model spans 110°E to 160°E, and 10°S to 45°S and is built from observations that have a five-layer representation which include sediments, basement, upper crust, middle crust and lower crust. However, the AuSREM crust is not explicitly layered and is defined by a regular grid of points with a depth discretization of 5 km. In the mantle, the grid is defined at 25-km intervals in depth and spans a geographic region from 105°E to 180°E, and 0°S to 50°S. Beyond this region and at depths greater than 350 km, AuSREM is linked to S40RTS (Ritsema et al. 2011), which is constructed from a large global dataset of surface, normal mode and body wave observations.

Seismic data exploited by AuSREM come from a wide variety of Australian-centric sources and include over 12,000 km of deep crustal reflection profiles, a number of major refraction experiments that used explosive sources between the 1960s and 1980s and a large number of passive portable seismic deployments that have sampled various parts of the continent since the early 1990s. The active source experiments have largely constrained the crustal architecture of the continent and have allowed major boundaries such as the Moho to be delineated. A degree of control over crustal properties is also possible, particularly from the refraction data, although in general P wave velocity is much better constrained than S wave velocity. A wide variety of techniques have been applied to the passive source data, which has provided valuable constraints on both crustal and mantle structure. One of the main sources of information comes from distant earthquake sources that surround the Australian plate, particularly from the north and east. The frequency of these earthquakes has allowed detailed images of mantle P wave and S wave velocity to be built up from sequences of portable deployments using both surface wave and body wave tomography. In the upper mantle, the primary source of information comes from surface wave tomography, although this is supplemented by body wave traveltime tomography which provides important constraints on the relationship between P and S wavespeeds. Receiver function studies, which provide important information on crustal and upper mantle discontinuities, have also been used. Ambient noise tomography, which exploits relatively high-frequency surface waves generated by oceanic and atmospheric disturbances, provides valuable constraints on crustal shear wave velocity variations, and is an important complement to the active source studies. A more detailed description of the data sources and how they are combined to form the AuSREM model can be found in Kennett and Salmon (2012).

Figure 2.2 illustrates the lateral heterogeneity that is inherent to the AuSREM model at crustal and mantle depths within the confines of the study area. The geometry of the Moho is also shown. Within the mantle, the first-order variation in P wavespeed is a gradual decrease from the NW to the SE, which reflects a transition from Precambrian cratonic Australia, to the younger fold belts of the Tasmanides, and then the thinned and possibly hotter and more enriched lithosphere beneath the eastern seaboard. Although the horizontal sampling of

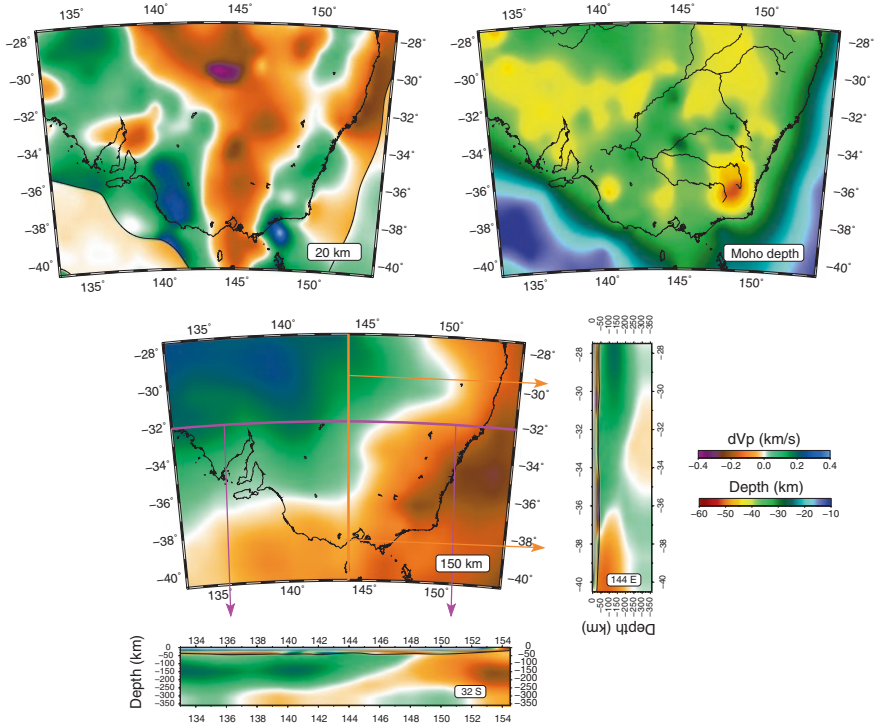


Fig. 2.2 P wave velocity variations (relative to laterally averaged 1-D model) and Moho geometry of the AuSREM model in the study region. Note that the depth scale refers only to the Moho depth variations displayed in plan view in the *top right*; all other horizontal and vertical slices display P wave velocity perturbations (dV_p). The velocity scale saturates at ± 0.4 km/s in order to properly visualize mantle variations; consequently, the full detail of crustal variations, particularly in cross-sectional view, is not represented in its entirety. Lateral discontinuities in velocity in the 20-km-depth slice are due to the undulating Moho, which becomes shallower than 20 km in several regions

AuSREM in this region is 0.5° in latitude and longitude, the maximum resolution in the mantle is of the order of 200–250 km, a limit inherited from the body and surface wave datasets used to constrain seismic structure at these depths. The Moho varies in depth from about 10 to 55 km, although it is almost entirely below 25 km depth inboard of the coastline. Nonetheless, variations in Moho depth beneath WOMBAT are sufficient to make sizable contributions to measured relative arrival time residuals, which should be accounted for in the inversion for 3-D velocity structure. The Moho is deepest beneath the Southern Highlands, which lie inboard of the east coast, and reflects the presence of a crustal root beneath up to 2 km of elevation. The shallow regions of the Moho lie offshore and are associated with the continental margin and the transition to oceanic lithosphere. The predominant strike of long-wavelength structures at 20 km depth (Fig. 2.2, top left) is N–S, which is largely consistent with the crustal elements plot shown in Fig. 2.1.

2.2 Data and Method

Data for this study are taken from the mainland stations of the WOMBAT transportable seismic array (Fig. 2.3), which has been in continuous operation in south-east Australia since 1998. To date, over 650 sites have been occupied during the course of 15 deployments, with individual arrays varying in size between 20 and 72 stations. Recording durations have also varied, with earlier arrays (e.g. LF98) operational for 4–5 months, while more recent deployments (e.g. EAL3) have run for more than 12 months. Prior to 2006, all seismometers used by WOMBAT were vertical component L4C sensors with a natural frequency of 1 Hz. Subsequent deployments have exclusively used 3-component Lennartz LE3Dlites which also have a natural frequency of 1 Hz. The use of short-period sensors has meant that the longer period component of teleseismic body waves and the bulk of surface wave energy from regional earthquakes, are not detected. However, teleseismic P phases such as direct P, PcP, ScP, PKiKP, PP, etc., are relatively ubiquitous in the long-term records, which makes them ideal for constraining relative variations in P wave velocity in the lithosphere beneath WOMBAT.

Figure 2.4 plots the locations of all 2985 teleseismic sources used in this study. Although earthquakes completely encircle WOMBAT, the azimuthal distribution varies quite considerably, with large concentrations lying to the north and east of Australia. In order to reduce the influence of uneven source distribution, we bin the data using the approach described in Rawlinson et al. (2011), which reduces the effective number of sources to 1115. The adaptive stacking method of Rawlinson and Kennett (2004) is used to measure relative arrival time residuals on a source by source basis. For a particular phase, the ak135 global reference model

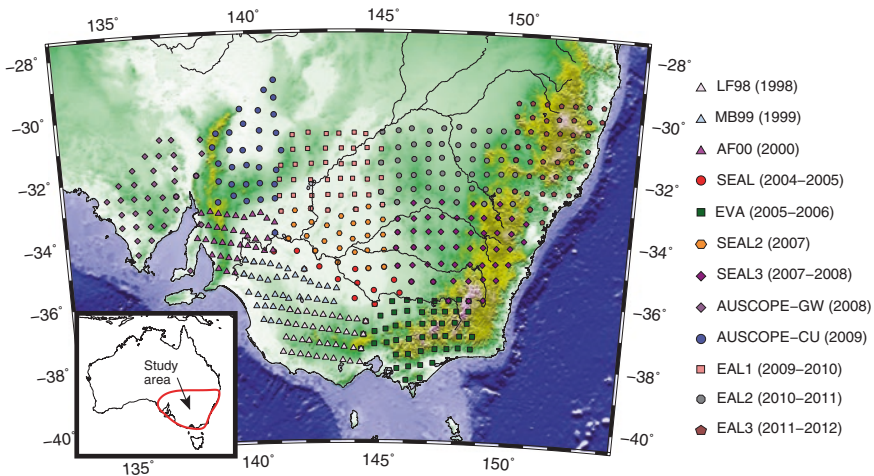


Fig. 2.3 Coverage of the WOMBAT transportable seismic array experiment in south-east mainland Australia

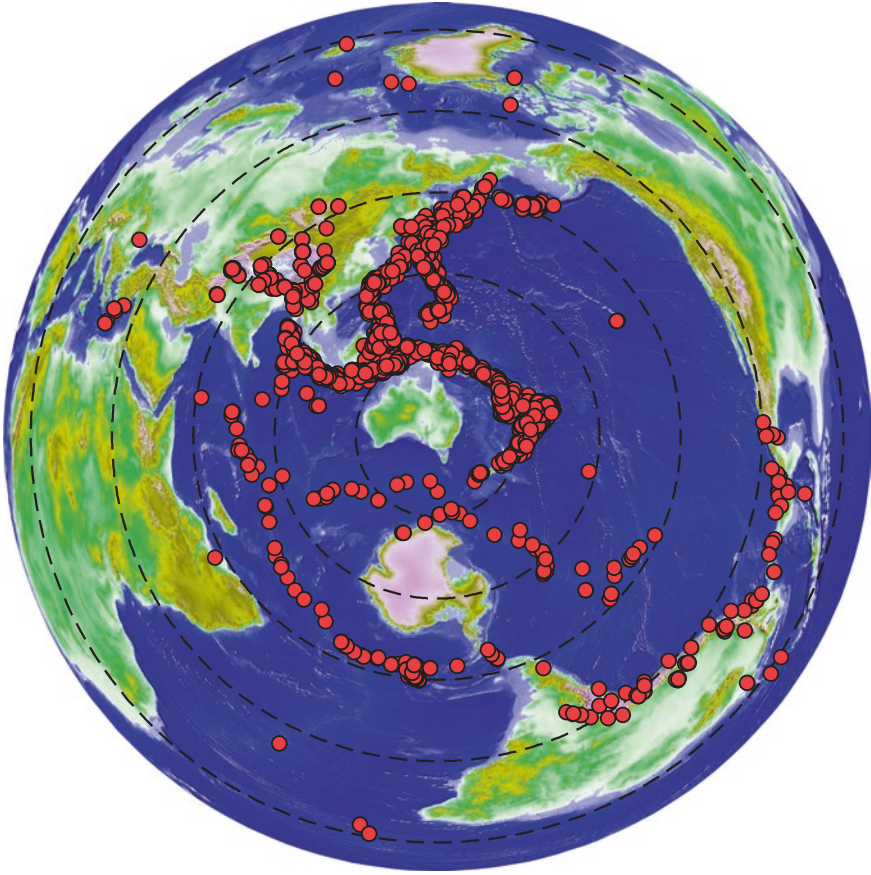


Fig. 2.4 Distribution of seismic sources used to constrain the 3-D P wave model. Concentric dashed circles are plotted at 30° intervals from the centre of WOMBAT

of Kennett et al. (1995) is used to remove the effect of trace move-out, which results in a preliminary alignment of the arriving wave trains at each station in the array. The remaining differences represent the arrival time residuals, which largely reflect the presence of lateral variations in structure beneath the array. Following preliminary alignment, all traces are linearly stacked, which produces a reference trace. Each trace is then optimally aligned with the reference trace using an L_p measure of misfit, where in our case $p = 3$ (see Rawlinson and Kennett 2004, for more details). The traces are then re-stacked and the alignment process repeated. This can be applied iteratively until convergence is achieved. The perturbation applied to each trace in order to achieve final alignment is a measure of the arrival time residual, from which the mean is removed on a source by source basis to help minimize temporal and spatial errors in source location, and long-wavelength variations in velocity in the deep mantle. In general, adaptive stacking is effective for teleseismic data, although problems can arise if the waveform is not coherent

across the array or lateral velocity variations are large enough to cause cycle skipping. Following binning of the data, the total number of arrival time residuals is 41,380.

The FMTOMO package (de Kool et al. 2006; Rawlinson and Urvoy 2006; Rawlinson et al. 2010b) is used to invert the measured traveltimes for variations in P wavespeed beneath the mainland component of the WOMBAT array. FMTOMO uses an eikonal solver known as the fast marching method (Sethian 1996; Rawlinson and Sambridge 2004a, b) to solve the forward problem of source–receiver traveltimes prediction, and a subspace inversion method (Kennett et al. 1988) to adjust model parameters in order to satisfy the data. The subsurface can be characterized by both smooth variations in wavespeed and discontinuities, which allows interfaces such as the Moho to be explicitly included. Phases can be composed of any number of reflection and refraction branches, and sources may be local or teleseismic. This level of flexibility means that FMTOMO can be used with reflection, wide-angle, local earthquake and/or teleseismic data. Model unknowns that can be constrained include velocity, interface depth and source location. Although FMTOMO could be used for quasi-global applications (it is written in spherical coordinates but does not allow for periodicity or the presence of the poles), its strength compared to conventional ray tracing lies in its ability to robustly compute two point traveltimes in the presence of sizable lateral heterogeneity. At the global scale, lateral heterogeneities are not significant enough to strongly perturb ray paths, which means that iterative two-point ray tracing schemes such as pseudo-bending (Koketsu and Sekine 1998) are much more efficient. However, within the upper mantle and particularly the crust, departures from lateral homogeneity can be very large, which makes eikonal solvers such as fast marching much more attractive.

We define our 3-D model structure beneath WOMBAT with a crustal layer and a mantle layer, separated by an undulating Moho. P wave variations in the crust and Moho depth variations are defined by AuSREM (Kennett and Salmon 2012) and are not permitted to vary during the inversion, since the shallow regions of the model are poorly constrained by the data. Although it would be possible to simultaneously invert for crust and upper mantle structure, we are unlikely to achieve any advantage as there is no crossing ray path coverage in the crust owing to the ~50-km station separation and use of teleseismic phases. Of particular concern would be trying to manage the trade-off between perturbations in crustal velocity and uppermost mantle velocity across the Moho discontinuity. The AuSREM mantle model (Kennett et al. 2013) defines initial P wave velocities in the mantle, which are subsequently adjusted during the inversion process. The complete model is defined by a total of 459,000 velocity nodes and 7650 interface nodes. During the iterative nonlinear inversion process, the data misfit component of the objective function is based on the difference between the predictions through the current model and the ak135 reference model (with receivers at zero elevation); thus, contributions to the measured residuals from both AuSREM and variations in receiver elevations are accounted for. The appropriate level of damping and smoothing regularization is determined by examining trade-off curves between data fit, model smoothness and model perturbation (see Rawlinson et al. 2006a, b, for details);

ideally, the optimum model is one that is as smooth and as close to the initial model as possible but still satisfies the data. The results of the synthetic testing shown in the next section help to illustrate the effect of the imposed regularization.

The use of FMTOMO together with AuSREM allows us to address several weaknesses in the traditional teleseismic tomography method. First, by explicitly including crustal and Moho structure, contributions to measured arrival time residuals from shallow unresolved structure are accounted for. The significant lateral heterogeneity in crustal velocity and thickness beneath WOMBAT (Fig. 2.2) has the potential to impart traveltimes perturbations of a similar magnitude to those generated by lateral perturbations in the upper mantle. As such, a crustal correction is mandatory for the reliable recovery of deep structure. Traditionally, this has been done using station correction terms that are treated as unknowns in the inversion (Frederiksen et al. 1998; Graeber et al. 2002; Rawlinson et al. 2006b), but the potential trade-off with mantle velocity perturbations can be difficult to quantify. Due to this difficulty, the use of a priori crustal models is becoming more popular (Waldhauser et al. 2002; Martin et al. 2005, Lei and Zhao 2007, Rawlinson et al. 2010b). Another weakness of teleseismic tomography is its reliance on relative arrival time residuals. Although absolute arrival time residuals could be used, contributions from source time uncertainty and structure outside the model region would negate any potential advantage. When using data from multiple arrays that do not record simultaneously, the removal of the mean on a source by source basis means that residuals from one array are not comparable to those from another unless the laterally averaged velocity structure beneath each array is identical. If this is not the case, then long-wavelength structure with a scale length similar to or larger than the aperture of the array will be lost. This phenomenon is explained in more detail in Evans and Achauer (1993), Rawlinson et al. (2011, 2013) and can be remedied in seismic tomography by using a starting model that contains the long-wavelength information that would otherwise be lost. Hence, by including the AuSREM mantle model in the initial model used by FMTOMO, we hope to end up with a final model that captures both the short- and long-wavelength features of the upper mantle. The principle assumption we are working with here is that the AuSREM model is correct; errors in crustal velocity will result in the introduction of artefacts into the recovered mantle structure, while errors in mantle velocity will translate as errors in the absolute velocities of the recovered model and, potentially, the larger scale patterns of lateral heterogeneity that extend between adjacent arrays.

2.3 Results

2.3.1 *Synthetic Tests*

Synthetic reconstruction tests are the most commonly used approach for assessing solution robustness for large tomographic inverse problems (Rawlinson et al. 2010a). Rather than directly quantifying solution uncertainty, this approach

essentially measures how variations in data coverage influence the recovery of structure (Rawlinson et al. 2010a). To do so, a synthetic dataset is constructed by solving the forward problem in the presence of a known model with preset velocity variations using the same sources, receivers and phase types as the field dataset. The inversion scheme is applied to this synthetic dataset, and a comparison of the recovered model and the true model provides insight into which regions of the model are well constrained by the data. A checkerboard pattern of alternating high and low velocities is often favoured as the input test model, as it makes visual comparison a relatively simple task. The limitations of synthetic reconstruction tests (Lévêque et al. 1993; Nolet 2008; Rawlinson et al. 2010a) are well known, such as the results varying according to the input structure used. Common alternatives include the calculation of formal estimates of posterior covariance and resolution from linear theory (Tarantola 1987), which provide quantitative measures of model uncertainty. However, these too suffer from several limitations such as decreasing validity with increasing nonlinearity of the inverse problem; inversion of a potentially very large matrix, although approximation methods have been developed to overcome this problem (Zhang and McMechan 1995; Zhang and Turber 2007); implicit regularization imposed by the chosen parameterization not being accounted for; a priori model covariance and data uncertainty usually poorly known. This coupled with the use of variable damping and smoothing often make the absolute value of posterior uncertainty rather meaningless. Rawlinson et al. (2010a, b) perform numerical experiments to show that the usefulness of synthetic reconstructions and posterior covariance and resolution estimates appear similar. In recent years, a number of other methods for assessing solution reliability of large tomographic systems have emerged, including dynamic objective functions (Rawlinson et al. 2008), generalized ray density tensors (Fichtner and Trampert 2011) and indirect methods for computing the resolution operator (MacCarthy et al. 2011; Trampert et al. 2013).

Here, we carry out two synthetic tests to help assess the reliability of P wavespeed patterns recovered in the mantle (Fig. 2.5). The first is a checkerboard reconstruction test in which the input checkerboard pattern is restricted to the mantle, where it is superimposed on the AuSREM P wave model (see Fig. 2.5a). Crustal P wave velocity structure and Moho geometry are defined by AuSREM and have not been perturbed. The peak amplitudes of the checkerboard anomalies are ± 0.4 km/s, which are similar to the peak amplitudes of velocity anomalies recovered from the WOMBAT dataset, as will be shown in the next section. The synthetic dataset that is generated from the model shown in Fig. 2.5a is contaminated with Gaussian noise with a standard deviation of 59 ms in order to simulate the noise content of the observational dataset, as estimated by the adaptive stacking procedure. Figure 2.5b shows horizontal and vertical slices through the recovered or output model that can be compared directly with Fig. 2.5a. Overall, the recovery of the checkerboard pattern is good within the horizontal bounds of the receiver array. Smearing is present towards the edge of the model where crossing ray path coverage is less dense. There is also more smearing in the N–S direction as a consequence of the source distribution (Fig. 2.4), which results in many more

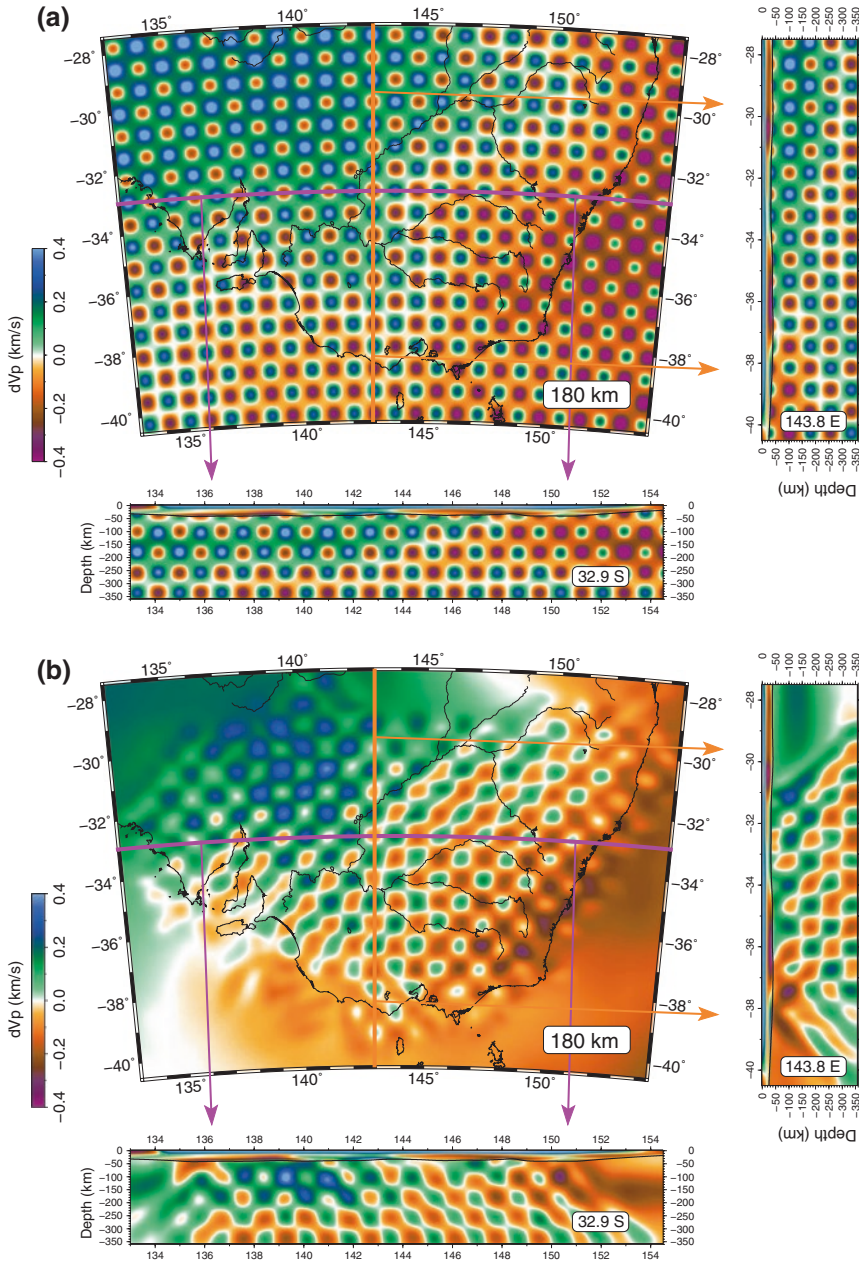


Fig. 2.5 Results of the synthetic checkerboard reconstruction test. **a** Input model; **b** recovered model. Velocity perturbation is relative to a laterally averaged 1-D model

paths impinging on the model from the north compared to the south. Moreover, the amplitudes of anomalies also tend to be underestimated, a feature typical of inversions that are regularized using smoothing and damping (Rawlinson et al. 2010a). However, the results do indicate that overall, the path coverage is sufficient to constrain features with a scale length upwards of 50 km within the horizontal bounds of the receiver array, although some caution is needed when interpreting the geometry of anomalies in the N–S direction. It also appears that structural recovery is uniformly good between the Moho and the base of the model at approximately 350 km depth.

In addition to the checkerboard reconstruction test, we also carry out a synthetic test in which the input anomalies are random patterns with a Gaussian distribution and standard deviation of 0.3 km/s. Compared to a checkerboard test,

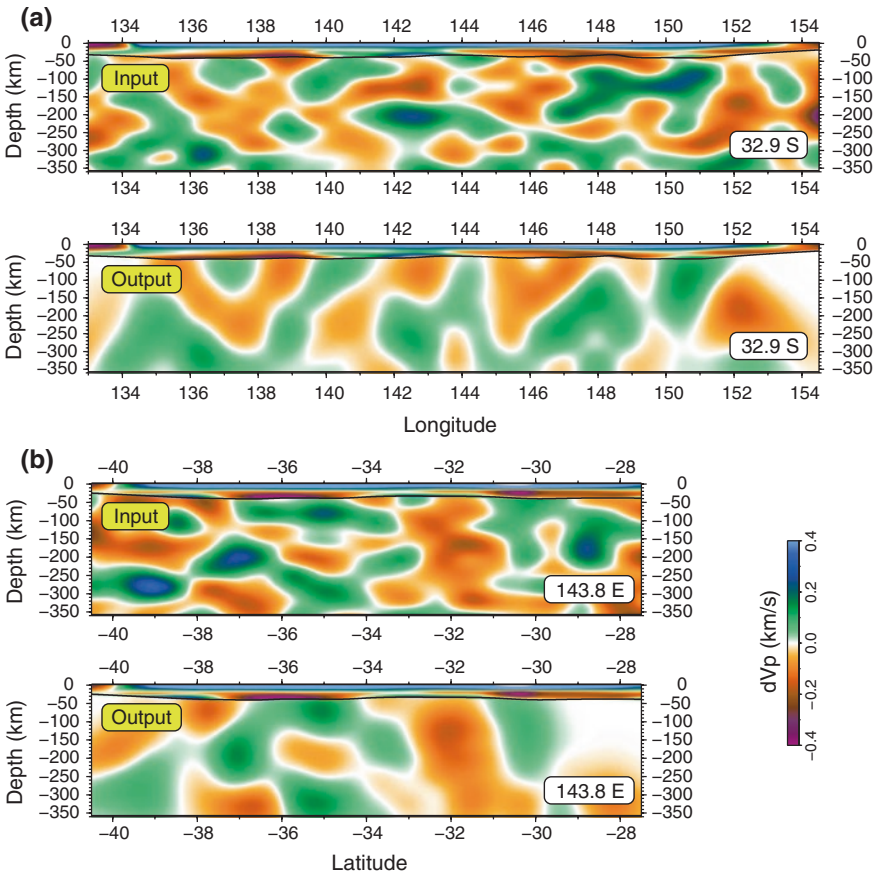


Fig. 2.6 Results of the synthetic reconstruction test using random velocity patterns with a Gaussian distribution. Vertical sections are taken at the same locations as shown in Fig. 2.5 checkerboard test. **a** E–W slice; **b** N–S slice. Velocity perturbation is relative to a laterally averaged 1-D model

this has the advantage that there is no regularity to the velocity variations and a range of scale lengths are present, which helps assess the extent of smearing. Figure 2.6a, c show cross sections through the input model, while Fig. 2.6b, d shows the corresponding output. As with the checkerboard model, Gaussian noise with a standard deviation of 59 ms has been added to the synthetic dataset to simulate the picking uncertainty associated with observational dataset. In comparing the input and output, the presence of vertical smearing of structure is the most obvious artefact of the recovery. This effect is typical in teleseismic tomography due to the steep inclination angles of impinging ray paths and imposes a limit on the extent to which vertical continuity of structure can be inferred.

2.3.2 *P Wave Velocity Structure Beneath South-east Australia*

Figures 2.7 and 2.8 show a series of horizontal and vertical slices through the final P wave velocity model that is obtained from inversion of the WOMBAT teleseismic dataset. The horizontal slices (Fig. 2.7) show that both short- and

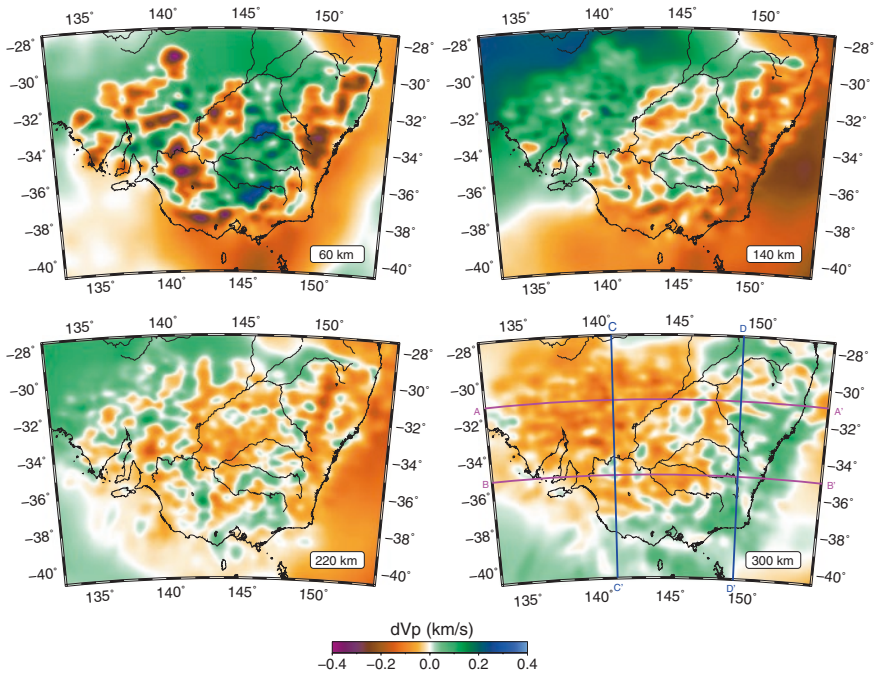


Fig. 2.7 Horizontal slices through the final WOMBAT teleseismic model. Velocity perturbation is relative to a laterally averaged 1-D model. Thick magenta and blue lines superimposed on the 300-km-depth slice (*bottom right*) denote locations of vertical slices shown in Fig. 2.8

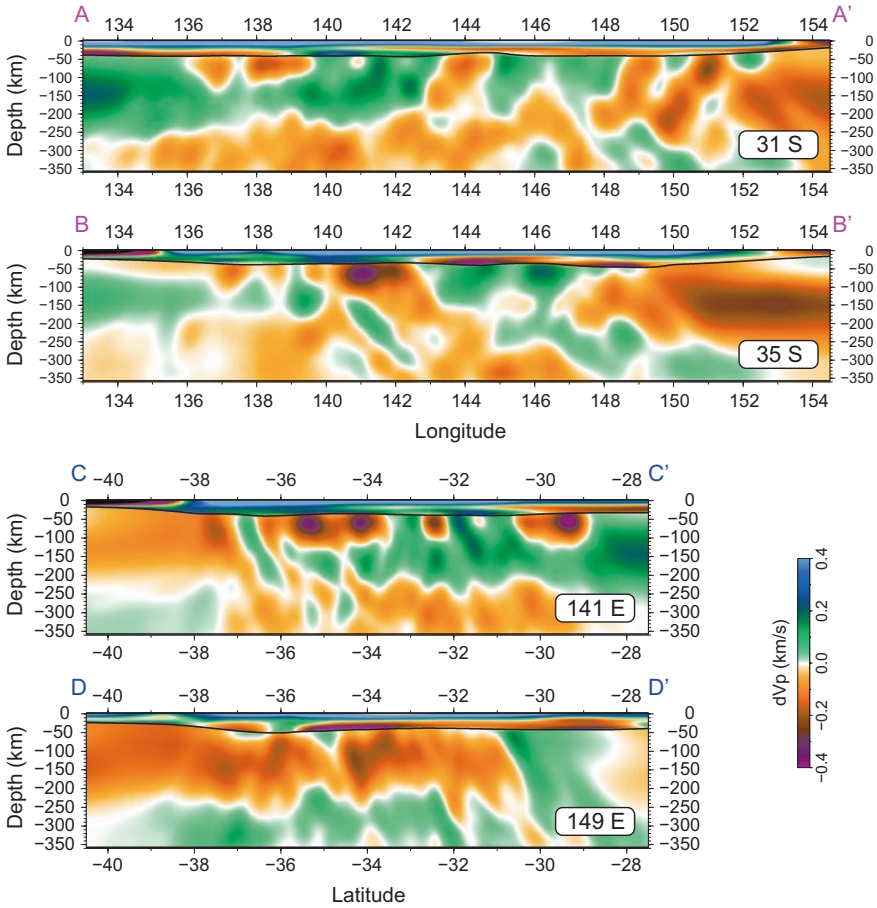


Fig. 2.8 Vertical slices through the final WOMBAT teleseismic model. Velocity perturbation is relative to a laterally averaged 1-D model. Refer to Fig. 2.7 for slice locations in plan view

long-wavelength patterns of lateral heterogeneity change markedly with depth. In the uppermost mantle at 60 km depth, the amplitude of anomalies is larger compared to the slices at greater depth; this may in part be due to less crossing path coverage, but it does make sense to have a more heterogeneous mantle in the immediate proximity of a very heterogeneous crust, given that the Moho does not necessarily represent a discontinuity in processes (e.g. deformation, intrusions, chemical alteration etc.). At 140 km depth, the general trend is a decrease in wavespeed to the south-east, which probably represents a decrease in the thickness of the continental lithosphere, which eventually transitions to oceanic outboard of the coastline. At 220 km depth, there is still evidence of higher wavespeeds in the north-west that are associated with Australia's cratonic interior, but by 300 km

depth, this is no longer the case. In fact, compared to the slice at 120 km depth, the trend is somewhat reversed, with higher velocities in the south-east and lower velocities in the north-west. The reason for this behaviour is unclear, but it may be related to a downwarp of the asthenosphere beneath the thicker parts of the continental lithosphere.

The two E–W and two N–S cross sections shown in Fig. 2.8 provide additional insight into the wavespeed variations beneath south-east Australia. In general, there does not appear to be a strong anti-correlation between velocities on either side of the Moho, which would indicate that the data poorly constrain the uppermost mantle. Slice A–A' at 31°S (Fig. 2.8, top) clearly illustrates that velocity is on average higher in the west than in the east, and if one took the 0.0 km/s contour line (for example) as a proxy for the base of the lithosphere, then it appears to thin towards the east which is consistent with surface wave results (Fishwick et al. 2008). Where path coverage is poor or non-existent, the model defaults back to AuSREM, which is clearly the case in the eastern sector of slice B–B' at 39°S. Although there appears to be a low-velocity zone in this region, it should be remembered that the velocity variations are visualized as a perturbation from a 1-D laterally averaged version of the final model in order to remove the first-order effect of velocity increasing with depth, which would otherwise obfuscate the velocity anomalies. The N–S slices (Fig. 2.8, bottom) show some evidence of N–S smearing; for example, the north-dipping high-velocity anomaly at about 37°S in slice C–C' may in fact be more vertical than the plot suggests.

Variations in mantle P wave velocity are a function of temperature, composition, grain size, melt and water content, and seismic data alone cannot discriminate between contributions from these separate factors. Consequently, there is growing interest in directly inverting multiple geophysical observables for the thermochemical state of the mantle (Khan et al. 2007, 2011; Afonso et al. 2008, 2013a, b; Simmons et al. 2009; Cammarano et al. 2011). However, in the absence of such methods and data, it is still possible to make reasonable inferences regarding the relationship between seismic velocity and physical and chemical properties of the mantle. Temperature appears to be a dominant factor, with a 1 % perturbation in velocity caused by as little as a 100 °C change in temperature (Cammarano et al. 2003). Nevertheless, the influence of composition has been argued to be equally as great in some circumstances, with realistic changes in composition producing anything between 1 and 5 % velocity variation (Griffin et al. 1998). Within the Australian continent, Faul and Jackson (2005) argue that lateral velocity variations can be explained by reasonable changes in temperature: thus, older cratonic Australia is simply colder than the younger warmer Tasmanides, which are characterized by lower velocities. More recently, Dalton and Faul (2010) found that while lateral variations in seismic velocity in the upper mantle are largely controlled by temperature variations in dry melt-free olivine, temperature alone cannot explain the high velocities that are sometimes observed above 200 km depth, particularly in cratonic regions. One possible explanation for this is the presence of chemically depleted lithosphere (higher Mg#), which will have the effect of increasing velocity.

2.4 Discussion and Conclusions

Compared to previous teleseismic studies which exploit WOMBAT data to image the lithosphere beneath south-east Australia (Graeber et al. 2002; Rawlinson et al. 2006b, 2011, 2013; Clifford et al. 2008; Rawlinson and Kennett 2008; Fishwick and Rawlinson 2012), the work presented here uses a geographically more extensive dataset and explicitly accounts for crustal velocity variations, Moho structure and long-wavelength anomalies in the mantle by adopting AuSREM as the starting model. Although the tomography results contained in Rawlinson et al. (2013) use a similar dataset, a less sophisticated imaging technique is used which relies on station terms to account for near-surface structure. Consequently, we regard the tomography results presented in the current study to be the most reliable produced so far. That said, the broad-scale variations in wavespeed in regions which overlap with previous studies are in general agreement; this can be regarded as a positive sign when sequential studies are performed in the same region using increasingly large datasets and/or different tomographic imaging schemes (Fishwick and Rawlinson 2012).

Figure 2.9 shows a 120-km-depth slice with crustal element and gravity and magnetic lineament information from Fig. 2.1 superimposed, as well as several regions of interest marked as A, B, C, D and E. Alongside, this horizontal slice is an E–W cross section taken at 37.5°S, an E–W cross section taken at 32.5°S, and a N–S cross section taken at 144.0°E. Perhaps the most interesting feature of the 3-D model is anomaly A in south-western Victoria which underlies the Quaternary NVP. The NVP is an extensive (~15,000 km²) intraplate basaltic province which is characterized by extensive lava flows, scoria cones and small shield volcanos of tholeiitic to alkalic composition (Vogel and Keays 1997; Price et al. 1997). It represents the largest and youngest expression of Late Tertiary to Quaternary basaltic volcanism in Australia, with an estimated eruption volume of 20,000 km³ and ages as recent as 5 Ka (Johnson 1989). Arguably the most outstanding question surrounding the NVP is the nature of the mantle source that gave rise to its existence. There has been no recent extension, nor is there strong evidence for a mantle plume source (Demidjuk et al. 2007). In the latter case, the elongated shape of the province in the E–W direction appears at odds with a plume source lying beneath a rapidly N–NE migrating Australian plate; in fact, over the approximately 4.5 M year duration of the eruptive sequences which characterize the NVP, the Australian plate may have moved over 300 km northwards, assuming current plate motion. Furthermore, Demidjuk et al. (2007) point out that this region of the Australian plate is in a state of compression and that the subdued topographic uplift (order of 100 m) associated with the NVP appears more consistent with a shallow mantle source rather than one which originates deep in the mantle. Figure 2.9 clearly shows the presence of a low-velocity zone beneath the surface outcrop of the NVP, both in plan view and in cross-sectional view. We attribute these lower velocities to the presence of increased temperature and melt in the uppermost mantle that gave rise to the intraplate basaltic province at the surface.

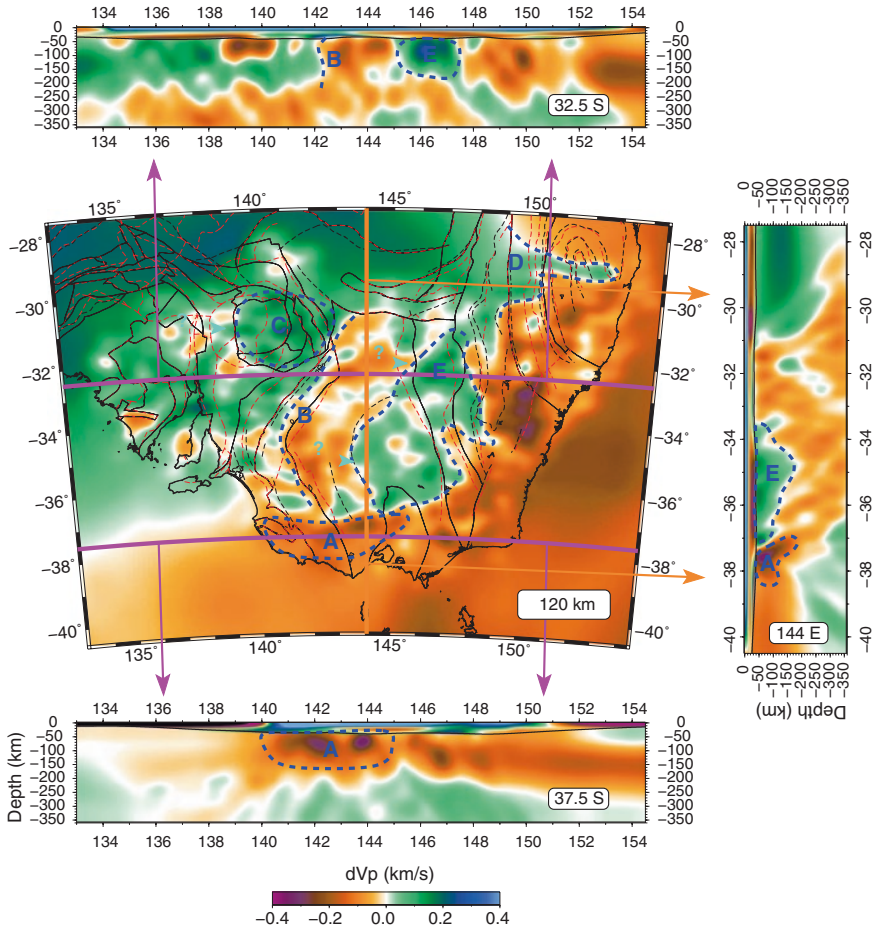


Fig. 2.9 Horizontal and vertical slices through WOMBAT teleseismic model with several features of interest highlighted in blue. See text for discussions of anomaly A, B, C, D and E

Both cross sections conclusively show that the low-velocity zone—and by inference the mantle source of the NVP—does not extend below approximately 200 km depth, which appears to rule out the possibility of a plume source. The N–S cross section (Fig. 2.9, right) shows that the low-velocity zone beneath the NVP appears to dip slightly to the north, something which can also be seen in the 60- and 140-km-depth sections of Fig. 2.7. However, as the checkerboard tests show (Fig. 2.5), the irregularity of the ray path geometry may contribute to this effect.

One alternative to a mantle plume source for the NVP that has been suggested previously is that of edge-driven convection (Demidjuk et al. 2007), in which the topography of the base of the lithosphere combines with its rapid northward migration to drive a localized convection process. More specifically, Demidjuk et al. (2007) argue that, based on surface wave tomography results, a step in

lithospheric thickness occurs some 300–400 km north of the NVP with a trend of $\sim 80^\circ\text{E}$. This inference is based on a N–S contrast from higher to lower velocities at 125 km depth. They use numerical modelling (assuming a 100 km change in lithospheric thickness across the step) to show that a convective cell with an E–W axis can be driven by the existence of such a step in the presence of a northward moving plate. Our results (Fig. 2.9) clearly reveal a N–S change from higher to lower velocities at around $30^\circ\text{--}31^\circ\text{S}$, which could be interpreted as a change from thicker to thinner lithosphere, although a change in lithospheric composition and temperature may also induce such a velocity contrast. Perhaps more significantly, sizable velocity anomalies exist to the south of this “step”, which suggest that a simple convection model involving a single marked change in lithospheric thickness probably does not tell the whole story. Further work is evidently needed to combine these new seismic results with those from geochemistry and geodynamic modelling in order to refine our understanding of melting processes in the upper mantle.

In addition to the low-velocity zone beneath the NVP, low velocities also encroach several 100-km inboard of the east coast. Unlike the NVP, these low velocities are likely a consequence of lithospheric thinning associated with the adjacent passive margin, which has brought the sublithospheric mantle closer to the surface. However, it is also possible that extensive Cenozoic volcanism in the region (Johnson 1989), which is a manifestation of processes in the mantle, may have effected the compositional and thermal structure of the lithosphere. Given that much of this volcanism occurred between 10 and 30 Ma, it is unclear whether remnant temperature anomalies or melt may contribute to the lower velocities, as is the case for the much younger NVP.

The extent of Precambrian continental basement beneath the southern Tasmanides has been the ongoing focus of much attention over the last few decades (Rutland 1976; Chappell et al. 1988; VandenBerg 1999; Foster and Gray 2000; Willman et al. 2002; Spaggiari et al. 2004; Glen 2005; Glen et al. 2009; Glen 2013), not only with regard to how far east parts of cratonic Australia—possibly deformed during the formation of the Tasmanides—may underpin the Tasmanides, but the extent to which Precambrian continental fragments may have become entrained within the Palaeozoic orogenic process. Feature B in Fig. 2.9, which highlights a W–E contrast from higher to lower velocities, has a very similar trend to the crustal element boundary in Fig. 2.1, and we interpret this change to mark the approximate location of the eastern boundary of the Delamerian Orogen in the upper mantle. It has been argued that the origin of the substrate in this south-east region of the Delamerian Orogen is dominantly Palaeozoic oceanic (Glen 2005, 2013; Foden et al. 2006), yet at upper mantle depths it appears to have a different seismic structure to the adjoining Lachlan Orogen, which is widely regarded as Palaeozoic oceanic in origin (Foster and Gray 2000, Spaggiari et al. 2003; Foster et al. 2009; Glen 2013). This difference could be attributed to thicker lithosphere beneath the Delamerian Orogen compared to the Lachlan Orogen, and/or involve some compositional change. Handler and Bennet (2001) use Re–Os isotopic data from spinel peridotite xenoliths to show that the eastern edge of the Precambrian interior (at upper mantle depths) of Australia appears to extend as far

east as the Delamerian–Lachlan boundary at the surface. Our seismic tomography results appear to be consistent with this finding, although it may be that remnant Proterozoic continental mantle lithosphere—perhaps a product of passive margin formation—underlies or is intermixed with Palaeozoic oceanic crust or lithosphere, respectively. If this was the case, it would help reconcile what is observed at the surface with what is inferred at depth.

Another distinctive feature of the Delamerian Orogen is the Palaeoproterozoic–Mesoproterozoic Curnamona province in the north, which recent evidence suggests formed part of a coherent and contiguous crustal system with the Gawler Craton by the late Palaeoproterozoic to early Mesoproterozoic (Hand et al. 2008). In Fig. 2.8, there is a clear zone of elevated velocity beneath the Curnamona province (denoted as anomaly C), which is characteristic of ancient depleted lithosphere (Dalton and Faul 2010). Although one could argue that translating this anomaly some 250–300 km westward would slot it back into the re-entrant in the Gawler Craton, it is a little difficult to substantiate such a claim on the basis of seismic structure alone.

North of about 30°S, and eastwards as far as 147°E, the lithosphere at 120 km depth (Fig. 2.9) is characterized by the same high velocities that are found throughout much of cratonic central and Western Australia. This strongly implies that the Thomson Orogen is underlain by Precambrian continental crust, a result that appears consistent with the recent results of Glen et al. (2013), who argue that the lower crust beneath the southern Thomson Orogen comprises continental crust that is older than 580 Ma. Anomaly D in Fig. 2.9, which lies to the east of the high-velocity substrate of the southern Thomson Orogen, indicates that a high-velocity salient protrudes beneath the New England Orogen and appears to terminate beneath the eastern edge of the New England oroclinal folds. Whether this “finger” is actually so narrow in the N–S direction is difficult to answer due to the lack of resolution in the northernmost part of the model, but given the much lower velocities to the south, there is evidently a very strong N–S change in lithospheric character that takes place beneath the New England oroclinal folds. The New England oroclinal folds were formed between 310–230 Ma as a result of deformation applied to a pre-Permian convergent margin assemblage (Cawood et al. 2011; Rosenbaum 2012). The exact mechanism of formation is still unclear, with several recent tectonic models invoking different convergent margin behaviour to explain the existence of a northern and southern oroclinal fold pair. For example, Cawood et al. (2011) propose a model in which buckling about a vertical axis is accomplished by having the southern part of the convergent margin elements moving northwards as a result of oblique sinistral strike-slip motion between the Pacific and Gondwana plates, with the northern part pinned relative to cratonic Gondwana. Other models appeal to irregularities along strike of the convergent margin, such as amplified buckle folds (Glen and Roberts 2012) or differential subduction roll-back (Rosenbaum 2012). It is unclear whether the spatial correlation of the New England oroclinal folds and the high-velocity salient is coincidental or provides insight into the localization of the oroclinal folds. Indeed, if the higher velocities do point to

possibly thicker and stronger lithosphere, then this may have the opposite effect of resisting such severe deformation. Of greater certainty is that anomaly D in Fig. 2.9 represents the presence of Precambrian lithosphere of continental origin beneath the New England Orogen. This has been inferred to exist on the basis of Re–OS analysis of peridotitic xenoliths (Powell and O'Reilly 2007), seismic reflection data (Finlayson 1993) and Geochronology (Hensel et al. 1985).

Anomaly E in Fig. 2.9 spans the western, central and eastern subprovinces of the Lachlan Orogen and in some regions is characterized by velocities as high as those observed beneath the Curnamona province. The similarity in the geometry of the western margin of anomaly E and the east Delamerian margin indicated by transition zone B in Fig. 2.9 raises the possibility that the two regions were once joined, in which case anomaly E may represent lithosphere with a similar provenance to the eastern Delamerian Orogen. In the study by Hallet et al. (2005), the authors use potential field data to identify a new zone within the Lachlan Orogen which they call the Hay–Booligal Zone, and others have inferred to be a fragment of crust of continental origin (e.g. Musgrave and Rawlinson 2010). The southern half of anomaly E corresponds almost exactly with the location of the Hay–Booligal Zone at the surface; for instance, the western edge of the anomaly almost coincides with the curved magnetic lineament (black dashed line) which marks the near-surface boundary of the zone. Given the strong correlation in shape between the western edge of this anomaly and the geometry of anomaly B, it would appear more likely that the Hay–Booligal Zone is a rifted remnant of the east Gondwana margin (Glen 2013) than a more exotic microcontinent. The northern part of anomaly E lies beneath parts of the Ordovician Macquarie Arc, which various lines of evidence, including a lack of continent-derived detritus and the primitive nature of Pb isotopes, point to it forming as an intra-oceanic arc (Glen et al. 2011). This would rule out a Precambrian continental origin for the northern part of anomaly E; instead, the higher velocities that are observed may be the result of local thickening of oceanic lithosphere and magmatic intrusion.

While it appears that several high-velocity upper mantle bodies beneath the Tasmanides correlate quite well with the presence of crustal blocks of Precambrian continental origin, there is by no means a perfect match, as was demonstrated by the northern part of anomaly E which lies beneath the Macquarie Arc. Another example is the Selwyn Block, which has been inferred to lie beneath central Victoria (Cayley et al. 2002; Cayley 2011); in Fig. 2.9, there is no evidence of such a feature in the upper mantle. This may be due in part to the overprinting effects of the Newer Volcanics province, or the fact that near the southern limit of the WOMBAT array, resolution decreases as a consequence of reduced path coverage. Other possibilities include that the Precambrian mantle lithosphere is no longer present (e.g. due to delamination), or that the composition of the Selwyn Block lithospheric mantle is such that it is not characterized by anomalously high velocities in comparison with the surrounding Lachlan Orogen.

Acknowledgments This work was supported by Australian Research Council Discovery Grant DP120103673.

References

- Afonso JC, Fernández N, Ranalli G, Griffin WL, Connolly JAD (2008) Integrated geophysical-petrological modelling of the lithospheric-sublithospheric upper mantle: methodology and applications. *Geochem Geophys Geosyst* 9. doi:[10.1029/2007GC001834](https://doi.org/10.1029/2007GC001834)
- Afonso JC, Fullea J, Griffin WL, Yang Y, Jones AG, Connolly JAD, O'Reilly SY (2013a) 3D multi-observable probabilistic inversion for the compositional and thermal structure of the lithosphere and upper mantle. I: a priori petrological information and geophysical observables. *J Geophys Res* (in press)
- Afonso JC, Fullea J, Yang Y, Connolly JAD, Jones AG (2013b) 3D multi-observable probabilistic inversion for the compositional and thermal structure of the lithosphere and upper mantle. II: General methodology and resolution analysis. *J Geophys Res* (in press)
- Belousova E, Preiss W, Schwarz M, Griffin W (2006) Tectonic affinities of the Houghton Inlier, South Australia: U-Pb and Hf-isotope data from zircons in modern stream sediments. *Aust J Earth Sci* 53:971–989
- Berry RF, Steele DA, Meffre S (2008) Proterozoic metamorphism in Tasmania: implications for tectonic reconstructions. *Precambr Res* 166:387–396
- Bolt BA, Niazi M (1964) Dispersion of Rayleigh waves across Australia. *Geophys J Royal Astr Soc* 9:21–35
- Bolt BA, Doyle HA, Sutton DJ (1958) Seismic observations from the 1956 atomic explosions in Australia. *Geophys J Royal Astr Soc* 1:135–145
- Bowman R, Kennett BLN (1990) An investigation of the upper mantle beneath northwestern Australia using a hybrid seismograph array. *Geophys J Int* 101:411–424
- Bowman R, Kennett BLN (1993) The velocity structure of the Australian shield from seismic traveltimes. *Bull Seism Soc Am* 83:25–37
- Calvert CR, Walter MR (2000) The Late Neoproterozoic Grassy Group of King Island, Tasmania: correlation and palaeogeographic significance. *Precambr Res* 100:299–312
- Cammarano F, Goes S, Vacher P, Giardini D (2003) Inferring upper-mantle temperatures from seismic velocities. *Phys Earth Planet Inter* 138:197–222
- Cammarano F, Tackley P, Boschi L (2011) Seismic, petrological and geodynamical constraints on thermal and compositional structure of the upper mantle: global thermo-chemical models. *Geophys J Int* 187:1301–1318
- Cawood PA, Pisarevsky SA, Leitch EC (2011) Unraveling the New England orocline, East Gondwana accretionary margin. *Tectonics* 30. doi:[10.1029/2011TC002864](https://doi.org/10.1029/2011TC002864)
- Cayley R (2011) Exotic crustal block accretion to the Eastern Gondwana margin in the Late Cambrian-Tasmania, the Selwyn Block, and implications for the Cambrian-Silurian evolution of the Ross, Delamerian and Lachlan orogens. *Gondwana Res* 19:628–649
- Cayley R, Taylor DH, VandenBerg AHM, Moore DH (2002) Proterozoic—early Palaeozoic rocks and the Tyennan Orogeny in central Victoria: the Selwyn Block and its tectonic implications. *Aust J Earth Sci* 49:225–254
- Chappell BW, White AJR, Hine R (1988) Granite provinces and basement terranes in the Lachlan Fold Belt, Southeastern Australia. *Aust J Earth Sci* 35:505–521
- Clifford P, Greenhalgh S, Houseman G, Graeber F (2008) 3-d seismic tomography of the Adelaide fold belt. *Geophys J Int* 172:167–186
- Clitheroe G, Gudmundsson O, Kennett BLN (2000) The crustal thickness of Australia. *J Geophys Res* 105:13697–13713
- Conor CHH, Preiss WV (2008) Understanding the 1720–1640 Ma Palaeoproterozoic Willyama Supergroup, Curnamona province, Southeastern Australia: Implications for tectonics, basin evolution and ore genesis. *Precambr Res* 166:297–317
- Dalton CA, Faul UH (2010) The oceanic and cratonic upper mantle: Clues from joint interpretation of global velocity and attenuation models. *Lithos* 120:160–172
- De Jersey NI (1946) Seismological evidence bearing on crustal thickness in the southwest Pacific. University of Queensland, papers 3: no 2

- Debayle E (1999) *SV-wave azimuthal anisotropy in the Australian upper mantle: preliminary results from automated Rayleigh waveform inversion*. *Geophys J Int* 137:747–754
- Debayle E, Kennett BLN (2000) The Australian continental upper mantle: Structure and deformation inferred from surface waves. *J Geophys Res* 105:25423–25450
- de Kool M, Rawlinson N, Sambridge M (2006) A practical grid based method for tracking multiple refraction and reflection phases in 3D heterogeneous media. *Geophys J Int* 167:253–270
- Demidjuk Z, Turner S, Sandiford M, Rhiannon G, Foden J, Etheridge M (2007) U-series isotope and geodynamic constraints on mantle melting processes beneath the newer volcanic province in south australia. *Earth Planet Sci Lett* 261:517–533
- Direen NG, Crawford AJ (2003) The Tasman Line: where is it, what is it, and is it Australia's Rodinian breakup boundary? *Aust J Earth Sci* 50:491–502
- Doyle HA (1957) Seismic recordings of atomic explosions in australia. *Nature* 180:132–134
- Evans JR, Achauer U (1993) Teleseismic tomography using the ach method: theory and application to continental scale studies. In: Iyer HM, Hirahara K (eds) *Seismic tomography: theory and practice*. Chapman & Hall, London, pp 319–360
- Faul UH, Jackson I (2005) The seismological signature of temperature and grain size variations in the upper mantle. *Earth Planet Sci Lett* 234:119–134
- Fichtner A, Trampert J (2011) Resolution analysis in full waveform inversion. *Geophys J Int* 187:1604–1624
- Finlayson DM (1993) Crustal architecture across Phanerozoic Australia along the Eromanga-Brisbane geoscience transect: evolution and analogues. *Tectonophysics* 219:191–211
- Finlayson DM, Cull JP, Drummond BJ (1974) Upper mantle structure from the trans-Australia seismic survey (TASS) and other seismic refraction data. *J Geol Soc Aust* 21:447–458
- Finlayson DM, Collins CDN, Denham D (1980) Crustal structure under the Lachlan Fold Belt, Southeastern Australia. *Phys Earth Planet Inter* 21:321–342
- Finlayson DM, Collins CDN, Lock J (1984) P-wave velocity features of the lithosphere under the Eromanga Basin, Eastern Australia, including a prominent MID-crustal (Conrad?) discontinuity. *Tectonophysics* 101:267–291
- Finlayson DM, Collins CDN, Lukaszuk I, Chudyk EC (1998) A transect across Australia's southern margin in the Otway Basin region: crustal architecture and the nature of rifting from wide-angle seismic profiling. *Tectonics* 28:177–189
- Fishwick S, Rawlinson N (2012) 3-D structure of the Australian lithosphere from evolving seismic datasets. *Aust J Earth Sci* 59:809–826
- Fishwick S, Kennett BLN, Reading AM (2005) Contrasts in lithospheric structure within the Australian craton—insights from surface wave tomography. *Earth Planet Sci Lett* 231:163–176
- Fishwick S, Heintz M, Kennett BLN, Reading AM, Yoshizawa K (2008) Steps in lithospheric thickness within Eastern Australia, evidence from surface wave tomography. *Tectonics* 27. doi:[10.1029/2007TC002116](https://doi.org/10.1029/2007TC002116)
- Foden J, Sandiford M, Dougherty-Page J, Williams I (1999) Geochemistry and geochronology of the Rathjen Gneiss: implications for the early tectonic evolution of the Delamerian Orogen. *Aust J Earth Sci* 46:377–389
- Foden J, Elburg MA, Dougherty-Page J, Burt A (2006) The timing and duration of the Delamerian Orogeny: correlation with the Ross Orogen and implications for Gondwana assembly. *J Geol* 114:189–210
- Foster DA, Gray DR (2000) Evolution and structure of the Lachlan Fold Belt (Orogen) of Eastern Australia. *Ann Rev Earth Planet Sci* 28:47–80
- Foster DA, Gray DR, Spaggiari CV (2005) Timing of subduction and exhumation along the Cambrian East Gondwana margin and formation of Paleozoic back arc basins. *Geol Soc Am Bull* 117:105–116
- Foster DA, Gray DR, Spaggiari C, Kamenov G, Bierlein FP (2009) Palaeozoic Lachlan orogen, Australia; accretion and construction of continental crust in a marginal ocean setting: isotopic evidence from Cambrian metavolcanic rocks. *Geol Soc Lond Spec Publ* 318:329–349

- Frederiksen AW, Bostock MG, VanDecar JC, Cassidy JF (1998) Seismic structure of the upper mantle beneath the northern Canadian Cordillera from teleseismic traveltime inversion. *Tectonophysics* 294:43–55
- Gaina C, Müller D, Royer JY, Stock J, Hardebeck J, Symonds P (1998) The tectonic history of the Tasman Sea: A puzzle with 13 pieces. *J Geophys Res* 103:12413–12433
- Gibson GM, Morse MP, Ireland TR, Nayak GK (2011) Arc-continent collision and orogenesis in western Tasmanides: Insights from reactivated basement structures and formation of an ocean-continent transform boundary off western Tasmania. *Gondwana Res* 19:608–627
- Glen RA (2005) The Tasmanides of Eastern Australia. In: Vaughan APM, Leat PT, Pankhurst RJ (eds) *Terrane processes at the margins of Gondwana*. Geological Society, London, pp 23–96
- Glen RA (2013) Refining accretionary orogen models for the Tasmanides of eastern Australia. *Aust J Earth Sci* (in press)
- Glen RA, Roberts J (2012) Formation of Oroclines in the New England Orogen, Eastern Australia. *J Virtual Explorer* 43. doi:[10.3809/jvirtex.2012.00305](https://doi.org/10.3809/jvirtex.2012.00305)
- Glen RA, Scheibner E, Vandenberg AHM (1992) Paleozoic intraplate escape tectonics in Gondwanaland and major strike-slip duplication in the Lachlan Orogen of South-eastern Australia. *Geology* 20:795–798
- Glen RA, Percival IG, Quinn CD (2009) Ordovician continental margin terranes in the Lachlan Orogen, Australia: implications for tectonics in an accretionary orogen along the east Gondwana margin. *Tectonics* 28:doi:[10.1029/2009TC002446](https://doi.org/10.1029/2009TC002446)
- Glen RA, Saeed CDA, Quinn Griffin WL (2011) U-Pb and Hf isotope data from zircons in the Macquarie Arc, Lachlan Orogen: implications for arc evolution and Ordovician palaeogeography along part of the east Gondwana margin. *Gondwana Res* 19:670–685
- Glen RA, Quinn CD, Cooke DR (2012) The Macquarie Arc, Lachlan orogen, New South Wales; its evolution, tectonic setting and mineral deposits. *Episodes* 35:177–186
- Glen RA, Korsch RJ, Hegarty R, Costello RD, Saeed A, Poudjom Djomani RD, Costello RD, Griffin W (2013) Geodynamic significance of the boundary between the Thomson Orogen and the Lachlan Orogen, northwestern New South Wales and the implications for Tasmanide tectonics. *Austr J Earth Sci* (submitted)
- Graeber FM, Houseman GA, Greenhalgh SA (2002) Regional teleseismic tomography of the western Lachlan Orogen and the Newer Volcanic province, southeast Australia. *Geophys J Int* 149:249–266
- Griffin WL, O'Reilly SY, Ryan CG, Gaul O, Ionov DA (1998) Secular variation in the composition of subcontinental lithospheric mantle: geophysical and geodynamic implications. In: Braun J, Dooley J, Goleby B, van der Hilst R, Klitwijk C (eds) *Structure and evolution of the Australian continent*, vol 26. American Geophysical Union Geodynamic Series, pp 1–26
- Gunn PJ, Mackey TE, Yeates AN, Richardson RG, Seymour DB, McClenaghan MP, Calver CR, Roach MJ (1997) The basement elements of Tasmania. *Explor Geophys* 28:225–231
- Hallet M, Vassallo J, Glen R, Webster S (2005) Murray–Riverina region: an interpretation of bed-rock Palaeozoic geology based on geophysical data. *Q Notes Geol Surv NSW* 118:1–16
- Hand M, Reid A, Szpunar M, Direen n, Wade B, Payne j, Barovich K (2008) Crustal architecture during the early Mesoproterozoic Hiltaba-related mineralisation event: are the Gawler Range Volcanics a foreland basin fill? *MESA J* 51:19–24
- Handler MR, Bennet VC (2001) Constraining continental structure by integrating Os isotopic ages of lithospheric mantle with geophysical and crustal data: an example from Southeastern Australia. *Tectonics* 20:177–188
- Heintz M, Kennett BLN (2005) Continental scale shear-wave splitting analysis: investigation of seismic anisotropy underneath the Australian continent. *Earth Planet Sci Lett* 236:106–119
- Hensel HD, McCulloch MT, Chappell BW (1985) The New England Batholith: constraints on its derivation from Nd and Sr isotopic studies of granitoids and country rocks. *Geochim Cosmochim Acta* 49:369–384
- Hill D (1951) *Geology*. In: Mack G (ed) *Handbook of Queensland*. Australian Association for the Advancement of Science, Brisbane, pp 13–24

- Johnson BD (1973) A time term analysis of the data obtained during the Bass Strait upper mantle project (operation BUMP). *Bull Aust Soc Explor Geophys* 4:15–20
- Johnson RW (1989) *Intraplate volcanism in Eastern Australia and New Zealand*. Cambridge University Press, New York
- Kennett BLN (2003) Seismic structure in the mantle beneath Australia. In: Hillis RR, Müller RD (eds) *The evolution and dynamics of the Australian PLATE*, pp 7–23
- Kennett BLN, Abdullah A (2011) Seismic wave attenuation beneath the Australasian region. *Aust J Earth Sci* 58:285–295
- Kennett BLN, Bowman JR (1990) The structure and heterogeneity of the upper mantle. *Phys Earth Planet Inter* 59:134–144
- Kennett BLN, Salmon M (2012) AuSREM: Australian seismological reference model. *Aust J Earth Sci* 59:1091–1103
- Kennett BLN, Sambridge MS, Williamson PR (1988) Subspace methods for large scale inverse problems involving multiple parameter classes. *Geophys J* 94:237–247
- Kennett BLN, Engdahl ER, Buland R (1995) Constraints on seismic velocities in the earth from traveltimes. *Geophys J Int* 122:108–124
- Kennett BLN, Fishwick S, Reading AM, Rawlinson N (2004) Contrasts in mantle structure beneath Australia: relation to Tasman Lines? *Aust J Earth Sci* 51:563–569
- Kennett BLN, Fichtner A, Fishwick S, Yoshizawa K (2013) Australian seismological reference model (AuSREM): mantle component. *Geophys J Int* 192:871–887
- Khan A, Connolly JAD, MacLennan J, Mosegaard K (2007) Joint inversion of seismic and gravity data for lunar composition and thermal state. *Geophys J Int* 168:243–258
- Khan A, Boschi L, Connolly JAD (2011) Mapping the Earth's thermochemical and anisotropic structure using global surface wave data. *J Geophys Res* 116. doi:[10.1029/2010JB007828](https://doi.org/10.1029/2010JB007828)
- Koketsu K, Sekine S (1998) Pseudo-bending method for three-dimensional seismic ray tracing in a spherical earth with discontinuities. *Geophys J Int* 132:339–346
- Lambeck K, Penny C (1984) Teleseismic traveltime anomalies and crustal structure in central Australia. *Phys Earth Planet Inter* 34:46–56
- Lambeck K, Stephenson R (1986) The post-Palaeozoic uplift history of Southeastern Australia. *Aust J Earth Sci* 33:253–270
- Lei J, Zhao D (2007) Teleseismic P-wave tomography and the upper mantle structure of the central Tien Shan orogenic belt. *Phys Earth Planet Inter* 162:165–185
- Lévéque JJ, Rivera L, Wittlinger G (1993) On the use of the checker-board test to assess the resolution of tomographic inversions. *Geophys J Int* 115:313–318
- Li ZX (2001) An outline of the palaeogeographic evolution of the Australasian region since the beginning of the Neoproterozoic. *Earth Sci Rev* 53:237–277
- Li ZX, Baillie PA, Powell CM (1997) Relationship between northwestern tasmania and East Gondwanaland in the late cambrian/early ordovician: paleomagnetic evidence. *Tectonics* 16:161–171
- Lister GS, Etheridge MA (1989) Detachment models for uplift and volcanism in the Eastern Highlands, and their application to the origin of passive margin mountains. In: Johnson RW (ed) *Intraplate Volcanism in Eastern Australia and New Zealand*. Cambridge University Press, New York, pp 297–312
- Lister GS, Etheridge MA, Symonds PA (1986) Detachment faulting and the evolution of passive continental margins. *Geology* 14:246–250
- Lister GS, Etheridge MA, Symonds PA (1991) Detachment models for the formation of passive continental margins. *Tectonics* 10:1038–1064
- MacCarthy J, Brochers B, Aster R (2011) Efficient stochastic estimation of the model resolution matrix diagonal and generalized cross-validation for large geophysical inverse problems. *J Geophys Res* 116. doi:[10.1029/2011JB008234](https://doi.org/10.1029/2011JB008234)
- Martin M, Ritter JRR (2005) High-resolution teleseismic body-wave tomography beneath SE Romania—I. Implications for the three-dimensional versus one-dimensional crustal

- correction strategies with a new crustal velocity model. *Geophys J Int* 162:448–460 (the CALIXTO working group)
- Musgrave R, Rawlinson N (2010) Linking the upper crust to the upper mantle: comparison of teleseismic tomography with long-wavelength features of the gravity and magnetic fields of Southeastern Australia. *Explor Geophys* 41:155–162
- Nolet G (2008) A breviary of seismic tomography: imaging the interior of the earth and sun. Cambridge University Press, Cambridge
- Powell W, O'Reilly S (2007) Metasomatism and sulfide mobility in lithospheric mantle beneath Eastern Australia: implications for mantle ReOs chronology. *Lithos* 94:132–147
- Price RC, Gray CM, Frey FA (1997) Strontium isotopic and trace element heterogeneity in the plains basalts of the newer Volcanic province, Victoria, Australia. *Geochim Cosmochim Acta* 61:171–192
- Rawlinson N, Fishwick S (2012) Seismic structure of the Southeast Australian lithosphere from surface and body wave tomography. *Tectonophysics* 572:111–122
- Rawlinson N, Houseman GA, Collins CDN, Drummond BJ (2001) New evidence of Tasmania's tectonic history from a novel seismic experiment. *Geophys Res Lett* 28:3337–3340
- Rawlinson N, Kennett BLN (2004) Rapid estimation of relative and absolute delay times across a network by adaptive stacking. *Geophys J Int* 157:332–340
- Rawlinson N, Kennett BLN (2008) Teleseismic tomography of the upper mantle beneath the southern Lachlan Orogen, Australia. *Phys Earth Planet Inter* 167:84–97
- Rawlinson N, Kennett BLN, Heintz M (2006a) Insights into the structure of the upper mantle beneath the Murray Basin from 3D teleseismic tomography. *Austr J Earth Sci* 53:595–604
- Rawlinson N, Reading AM, Kennett BLN (2006b) Lithospheric structure of Tasmania from a novel form of teleseismic tomography. *J Geophys Res* 111. doi:[10.1029/2005JB003803](https://doi.org/10.1029/2005JB003803)
- Rawlinson N, Kennett B, Vanacore E, Glen R, Fishwick S (2011) The structure of the upper mantle beneath the Delamerian and Lachlan orogens from simultaneous inversion of multiple teleseismic datasets. *Gondwana Res* 19:788–799
- Rawlinson N, Pozgay S, Fishwick S (2010a) Seismic tomography: a window into deep Earth. *Phys Earth Planet Inter* 178:101–135
- Rawlinson N, Salmon N, Kennett BLN (2013) Transportable seismic array tomography in Southeast Australia: illuminating the transition from Proterozoic to Phanerozoic lithosphere. *Lithos* (submitted)
- Rawlinson N, Sambridge M (2004a) Multiple reflection and transmission phases in complex layered media using a multistage fast marching method. *Geophysics* 69:1338–1350
- Rawlinson N, Sambridge M (2004b) Wavefront evolution in strongly heterogeneous layered media using the fast marching method. *Geophys J Int* 156:631–647
- Rawlinson N, Sambridge M, Saygin E (2008) A dynamic objective function technique for generating multiple solution models in seismic tomography. *Geophys J Int* 174:295–308
- Rawlinson N, Tkalčić H, Reading AM (2010b) Structure of the Tasmanian lithosphere from 3-D seismic tomography. *Aust J Earth Sci* 57:381–394
- Rawlinson N, Urvoy M (2006) Simultaneous inversion of active and passive source datasets for 3-D seismic structure with application to Tasmania. *Geophys Res Lett* 33:doi:[10.1029/2006GL028105](https://doi.org/10.1029/2006GL028105)
- Reading AM, Kennett BLN (2003) Lithospheric structure of the Pilbara Craton, Capricorn orogen and Northern Yilgarn craton, Western Australia, from teleseismic receiver functions. *Aust J Earth Sci* 50:439–445
- Ritsema J, Deuss A, van Heijst HJ, Woodhouse JH (2011) S40RTS: a degree-40 shear velocity model for the mantle from new Rayleigh wave dispersion, teleseismic traveltimes and normal-mode splitting function measurements. *Geophys J Int* 184:1223–1236
- Rosenbaum G (2012) Oroclines of the southern New England Orogen, eastern Australia. *Episodes* 35:187–194
- Rutland RWR (1976) Orogenic evolution of Australia. *Earth Sci Rev* 12:161–196
- Salmon K, Kennett BLN, Saygin E (2012) Australian seismological reference model (AuSREM): crustal component. *Geophys J Int* 192:190–206

- Scheibner E (1974) Fossil fracture zones (transform faults), segmentation and correlation problems in the Tasman Fold Belt system. In: Demeade AK, Tweeddale GW, Wilson AF (eds) *Tasman geosyncline: a symposium in honour of Professor Dorothy Hill*, Geological Society of Australia, Brisbane, pp 65–98
- Scheibner E, Veevers JJ (2000) Tasman Fold Belt System. In: Veevers JJ (ed) *Billion-year earth history of Australia and neighbours in Gondwanaland*. GEMOC Press, Macquarie Univ, Sydney, pp 154–234
- Sethian JA (1996) A fast marching level set method for monotonically advancing fronts. *Proc Nat Acad Sci* 93:1591–1595
- Shaw RD, Wellman P, Gunn P, Whitaker AJ, Tarlowski C, Morse M (1996) Australian Crustal Elements based on the distribution of geophysical domains (1:5 000 000 scale map; version 2.4, ArcGIS dataset). Geoscience Australia, Canberra
- Shaw SW, Flood RH, Pearson NJ (2011) The New England Batholith of eastern Australia: evidence of silicic magma mixing from $^{176}\text{Hf}/^{177}\text{Hf}$ ratios. *Lithos* 126:115–126
- Simmons NA, Forte AM, Grand SP (2009) Joint seismic, geodynamic and mineral physical constraints on three-dimensional mantle heterogeneity: implications for the relative importance of thermal versus compositional heterogeneity. *Geophys J Int* 177:1284–1304
- Simons F, Zielhuis A, van der Hilst RD (1999) The deep structure of the Australian continent from surface wave tomography. *Lithos* 48:17–43
- Simons FJ, van der Hilst RD, Montagner JP, Zielhuis A (2002) Multimode Rayleigh wave inversion for heterogeneity and azimuthal anisotropy of the Australian upper mantle. *Geophys J Int* 151:738–754
- Spaggiari CV, Gray DR, Foster DA, McKnight S (2003) Evolution of the boundary between the western and central Lachlan Orogen: implications for Tasmanide tectonics. *Aust J Earth Sci* 50:725–749
- Spaggiari CV, Gray DR, Foster DA (2004) Lachlan Orogen subduction-accretion systematics revisited. *Aust J Earth Sci* 51:549–553
- Sutherland FL (1983) Timing, trace and origin of basaltic migration in eastern Australia. *Nature* 305:123–126
- Sutherland FL, Graham IT, Meffre S, Zwingmann H, Pogson RE (2012) Passive-margin prolonged volcanism, East Australian Plate: outbursts, progressions, plate controls and suggested causes. *Aust J Earth Sci* 59:983–1005
- Tarantola A (1987) *Inverse problem theory*. Elsevier, Amsterdam
- Thomas L (1969) Rayleigh wave dispersion in Australia. *Bull Seism Soc Am* 59:167–182
- Thomson BP (1970) A review of the Precambrian and lower Palaeozoic tectonics of South Australia. *Transactions of the Royal Society of South Australia* 94:193–221
- Trampert J, Fichtner A, Ritsema J (2013) Resolution tests revisited: the power of random numbers. *Geophys J Int* 192:676–680
- Underwood R (1969) A seismic refraction study of the crust and upper mantle in the vicinity of Bass Strait. *Aust J Phys* 22:573–587
- van der Beek PA, Braun J, Lambeck K (1999) Post-palaeozoic uplift history of Southeastern Australia revisited: results from a process-based model of landscape evolution. *Aust J Earth Sci* 46:157–172
- VandenBerg AHM (1999) Timing of orogenic events in the Lachlan orogen. *Aust J Earth Sci* 46:691–701
- van der Hilst R, Kennett B, Christie D, Grant J (1994) Project SKIPPY explores the lithosphere and mantle beneath Australia. *EOS, Trans Amer Geophys Union* 75:177–181
- Vogel DC, Keays RR (1997) The petrogenesis and platinum-group element geochemistry of the new Volcanic province, Victoria, Australia. *Chemical Geology* 136:181–204
- Wade C, Reid A, Wingate M, Jagodzinski Barovich K (2012) Geochemistry and geochronology of the c. 1585 ma Benagerie Volcanic Suite, southern Australia: relationship to the Gawler Range Volcanics and implications for the petrogenesis of a Mesoproterozoic silicic large igneous province. *Precambr Res* 206:17–35

- Waldhauser F, Lippitsch R, Kissling E, Ansorge J (2002) High-resolution teleseismic tomography of upper-mantle structure using an *a priori* three-dimensional crustal model. *Geophys J Int* 150:403–414
- Wellman P (1976) Gravity trends and the growth of Australia: a tentative correlation. *J Geol Soc Aust* 23:11–14
- Wellman P (1983) Hotspot volcanism in Australia and New Zealand: Cainozoic and mid-Mesozoic. *Tectonophysics* 96:225–243
- Willman CE, VandenBerg AHM, Morand VJ (2002) Evolution of the southeastern Lachlan Fold Belt in Victoria. *Aust J Earth Sci* 49:271–289
- Yoshizawa K, Kennett BLN (2004) Multimode surface wave tomography for the Australian region using a three-stage approach incorporating finite frequency effects. *J Geophys Res* 109. doi:[10.1029/2002JB002254](https://doi.org/10.1029/2002JB002254)
- Zhang H, Thurber CH (2007) Estimating the model resolution matrix for large seismic tomography problems based on Lanczos bidiagonalization with partial reorthogonalization. *Geophys J Int* 170:337–345
- Zhang J, McMechan GA (1995) Estimation of resolution and covariance for large matrix inversions. *Geophys J Int* 121:409–426
- Zielhuis A, van der Hilst RD (1996) Upper-mantle shear velocity beneath eastern Australia from inversion of waveforms from SKIPPY portable arrays. *Geophys J Int* 127:1–16

The Earth's Heterogeneous Mantle
A Geophysical, Geodynamical, and Geochemical
Perspective

Khan, A.; Deschamps, F. (Eds.)

2015, XV, 530 p. 166 illus., 142 illus. in color.,

Hardcover

ISBN: 978-3-319-15626-2